JOURNAL OF CATALYSIS 57, 222–230 (1979)

Thermal Decomposition of Gibbsite under Low Pressures

II. Formation of Microporous Alumina

J. ROUQUEROL, F. ROUQUEROL, AND M. GANTEAUME

Centre de Recherches de Microcalorimétrie et de Thermochimie du C.N.R.S., 26 Rue du 141e R.I.A., 13003 Marseille, France

Received October 12, 1976; revised October 9, 1978

The formation of microporous alumina from various gibbsite samples has been studied under conditions of controlled residual pressure and decomposition rate. The information obtained from thermal analysis, nitrogen adsorption, scanning calorimetry, and X-ray diffraction are consistent with a model in which the reaction interface advances parallel to the basal plane of the crystal, "drilling" micropores at the place of the "structural channels" of the gibbsite lattice and where the width of the micropores is controlled by the desorption stage.

INTRODUCTION

Our previous paper (*1*) dealt with the incomplete transformation of gibbsite $Al(OH)_3$ into boehmite AlO(OH) during the first step of its thermal decomposition under low pressures. The techniques used, especially the procedure of controlled decomposition-rate thermal analysis (C.R.T.A.) allowed us to show that boehmite formation could occur even in micron-size gibbsite crystals and even under a water vapor pressure as low as 0.1 Torr (1 Torr = 133.3 N m^{-2}). A careful study of the influence of the grain size, vapor pressure, and decomposition rate led us to the conclusion that the hydrothermal conditions necessary for the conversion into boehmite could be fulfilled even in a microcrystalline gibbsite but that they were closely controlled by the thickness of the surrounding crystalline "shell" and by the water desorption mechanism. During the course of the thermolysis, the rate of this reaction is progressively lowered (due to a thinning down of the gibbsite shell, responsible for a lowering of the internal pressure), whereas the rate of the second step (transformation of the unreacted gibbsite into porous alumina) is progressively increased (due to an increase of both the temperature and the extent of the external surface available to the reaction interface). The present paper is devoted to the study of this second step with the aim of extending the elegant work of de Boer *et al.* (*2–4*) (carried out under atmospheric pressure but with controlled humidity) and of Papée and Tertian (*5, 6*) (who stressed the influence of low water vapor pressures but who were restricted to the somewhat imprecise low-pressure conditions usually available at that time) to a more systematic study of the influence of the parameters which already proved to be so important in the understanding of the first step (residual vapor pressure in the 10^{-2}- to 10-Torr range, grain size, decomposition rate).

0021-9517/79/050222-09$02.00/0

EXPERIMENTAL

Since the samples and techniques used were described in Part I (*1*), we shall only point out a few important features.

Gibbsite Samples

Two samples consist of flat and distinct microcrystals (grain size: 0.2 and 1 μm, specific surface area: 15 and 5 $m^2\ g^{-1}$, respectively), whereas the third is an industrial sample, prepared by the Bayer process, and its grains (50–80 μm) result from the agglomeration of crystals of smaller size (specific surface area of this sample: 0.14 $m^2\ g^{-1}$).

Thermal Analysis Procedure

The method used (called above "C.R.T.A.") is a method where both the vapor flow from the sample and the vapor pressure above it are carefully controlled, so as to keep at a very low level the temperature and pressure gradients in the powder. An important result is a great synchronism in the thermal decomposition of all the individual grains of the powder, which highly simplifies the interpretation of any *macroscopic* determination (surface area, crystalline structure, enthalpy of reaction, apparent order of reaction).

Nitrogen Adsorption Determinations

The adsorption measurements were always performed *in the same sample bulb as the thermal analysis;* at any time of the thermal decomposition the heating and outgassing could be stopped, the sample bulb being then attached to a conventional volumetric apparatus for an adsorption run at the end of which a further thermal treatment could be carried out.

Calorimetric Determinations

To measure the enthalpy of dehydration of our samples we used a special assembly, associating differential microcalorimetry with the C.R.T.A. procedure (*20*).

TABLE 1

Differential Enthalpy of Dehydration of Gibbsite (kJ mol^{-1}) as a Function of Grain Size and Residual Pressure

Grain size (μm)	Residual pressure	
	0.04 Torr	1 Torr
0.2	88 ± 3	80 ± 2
1	84 ± 2	78.5 ± 1.5
50–80	80.5 ± 1.5	77 ± 2

RESULTS

We give in Fig. 1 several curves of thermal analysis (A), scanning calorimetry (B), and X-ray diffraction (C) for a 1-μm gibbsite sample decomposed under a self-generated water vapor pressure of 0.04 Torr [curves (I)] or 1 Torr [curves (II)]. The following features are worth stressing:

(a) On both thermal analysis curves of Fig. 1A, we notice that from point *b*1 to *c*, i.e., during the main part of the dehydration, the temperature is nearly constant; since, with our thermal analysis procedure, the rate of decomposition is also constant (here, 16 mg h^{-1} for a sample initially weighing 1.4 g), we may infer that the *apparent order of the reaction is zero* towards the amount of unreacted material; this fact had been observed by Goton and Eyraud (*7*) but had been more or less forgotten since conventional T.G., even at very low heating rates, is unable to give a similar result (*8*). This was obtained in conditions leading to a uniform decomposition in the whole sample, such as infinitely slow heating rate or controlled decomposition rate and pressure (*9*, *10*). In other words, this result is obtained when the synchronism of the decomposition throughout the sample is such as to allow measurements which are, at a macroscopic scale, really significant of what is

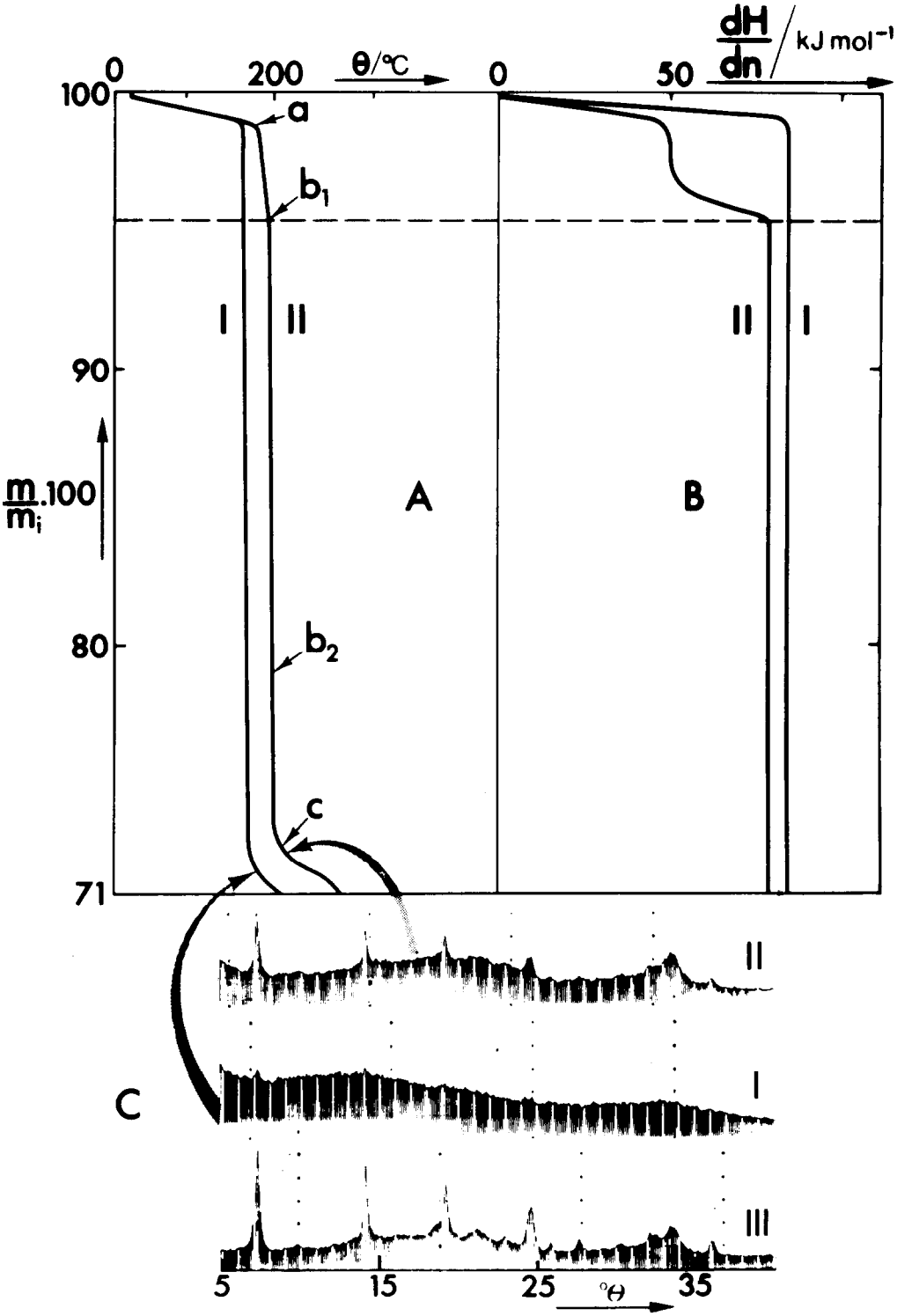
dH/dn kJ mol⁻¹
0
200
θ/°C
0
50
100
a
b1
I
II
II
I
90
m/mi .100
A
B
80
b2
c
71
C
II
I
III
5
15
25
°θ
35

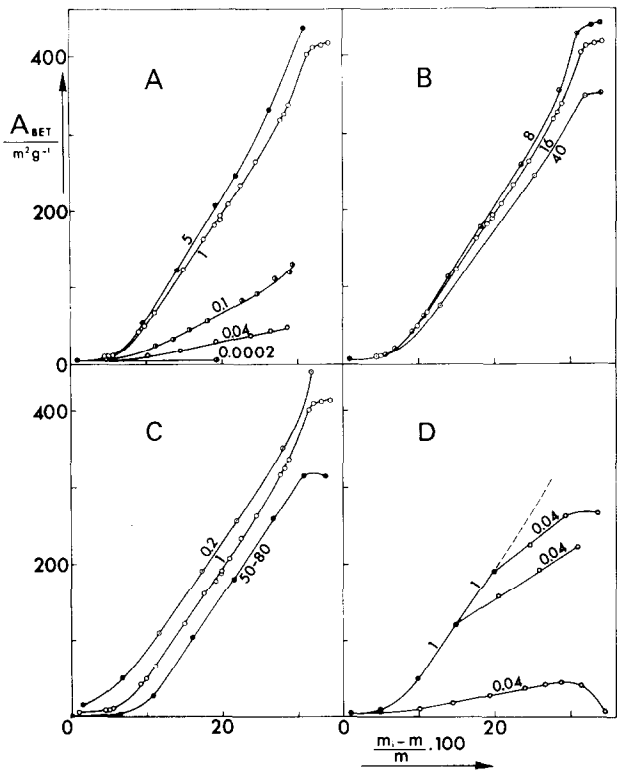

FIG. 2. Influence of three parameters on the development of the surface area accessible to nitrogen during the dehydration of gibbsite (initial mass of samples: 1.4 g). (A) and (D) Pressure (Torr); sample: 1 μm; rate: 16 mg h^{-1}. (B) Rate of decomposition (mg h^{-1}); sample: 1 μm; pressure: 1 Torr. (C) Grain size (μm); pressure: 1 Torr; rate: 16 mg h^{-1}.

happening at the microscopic scale, i.e., here, at the scale of the microcrystal.

(b) *The differential enthalpy of dehydration* (measured by simultaneous microcalorimetry and constant rate thermal analysis (C.R.T.A.)) reaches a constant level from the onset (point *b*1) of the second step of dehydration which we are now studying. As shown in Table 1, this level is dependent significantly on the residual water vapor pressure and on the grain size.

(c) The X-ray spectra for samples treated up to the neighborhood of point c show no trace of gibbsite, which is therefore completely decomposed at the end of the quasi-isothermal process. The alumina obtained under 0.04 Torr may be said to be amorphous [spectrum (I)] whereas a typical ρ alumina (*6*) with one diffraction peak at 1.40 Å is formed by decomposition under 1 Torr [spectrum (II)], but mixed with about 7% boehmite (cf. Fig. 3 in Part I); under atmospheric pressure [spectrum (III)] we obtain a mixture of boehmite (15%, cf. Fig. 5 in Part I) and χ alumina.

The curves plotted in Fig. 2 allow us to follow, in various conditions, the development of the specific surface area

FIG. 1. Thermal decomposition of the 1 μm gibbsite sample. (A) Thermal analysis curves (decomposition rate: 16 mg h^{-1}; initial mass: 1.4 g); (B) Curves of differential enthalpy of dehydration; (C) X-ray spectra at point C; (I) p = 0.04 Torr; (II) p = 1 Torr; (III) p = 1 atm.

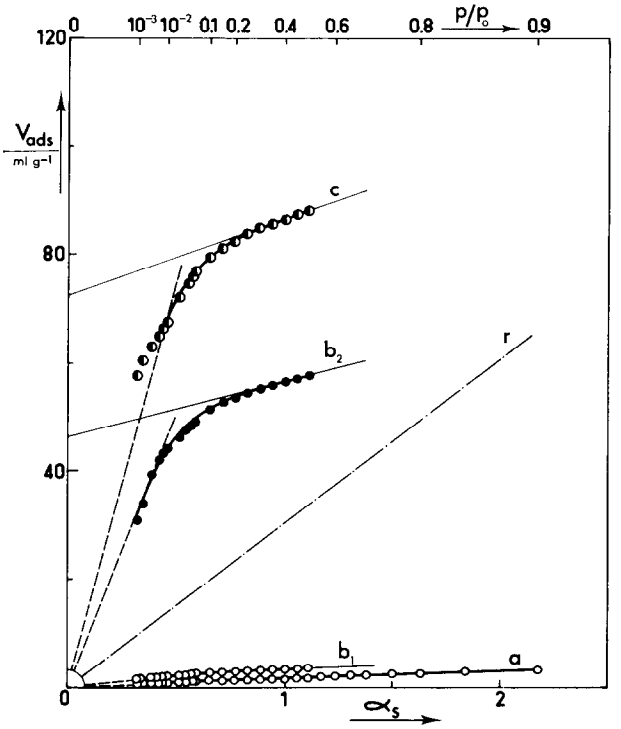

FIG. 3. α_s plots for samples represented by points *a*, b_1, b_2, and *c* in Fig. 1A.

accessible to nitrogen (BET method) during the thermal decomposition.

Figure 2A shows the striking influence of water vapor pressure; we see that *in all cases*, after a first stage during which dehydration takes place but without making any new surface available to nitrogen, *the BET surface area then increases linearly with the extent of decomposition.* The higher the residual pressure, the easier the distinction between the two stages and the easier also the interpretation of the first one, since we know (from Part I) that, for the highest pressures (1 and 5 Torr), it corresponds to boehmite formation in the core of the crystals. An extra experiment [T.G. associated with C.R.T.A., described in (*11*, *12*)] allowed us to carry out the decomposition of a 50-mg sample *under a residual pressure of only* 2×10^{-4} *Torr:* Under these conditions, *we could not detect any development of the surface area available to nitrogen,* which remained equal to 5 $m^2\ g^{-1}$.

Figure 2B shows a much smaller influence of the decomposition rate.

Figure 2C shows the influence of grain size. The larger the grain size, the lower the final available surface area. This is easily explained by the difference in the boehmite content (boehmite is still undecomposed in our experiments where thermal analysis curves similar to those given in Fig. 1A are followed up to point *c* only). On the other hand, as soon as boehmite is formed, *the three curves have the same slope,* indicating that the phenomenon responsible for the surface area increase is the same for the three samples.

Figure 2D shows *the effect of change of pressure at various stages* of gibbsite decomposition; as soon as the pressure is lowered from 1 to 0.04 Torr, the surface area curve follows a new path.

Figure 3 gives the α_s plots (*13*), derived from our nitrogen adsorption isotherms, for samples represented by points *a*, b_1, b_2, and *c* on the thermal analysis curve of Fig. 1A. Such plots are known to provide a means for detection of microporosity in a more straightforward manner than de Boer and Lippens' *t* plots (*14*). The standard nonmicroporous sample used here (α_s plot: dotted straight line *r*) is a Degussa "Aluminoxid" of 80 $m^2\ g^{-1}$. Whereas samples *a* (starting material) and b_1 (corresponding to the end of boehmite formation) are nonmicroporous with respect to nitrogen adsorption, samples b_2 and *c* give the typical α_s plot of a microporous sample. A similar α_s plot was given by Sing (*13*) for a gibbsite sample treated at 300°C. The slope of the second part of these α_s plots is taken as proportional to the nonmicroporous (or "external") surface area available to nitrogen and leads to external specific surface areas of 4.3, 7.5, 28, and 37 $m^2\ g^{-1}$ for samples *a*, b_1, b_2, and *c*, respectively. Since the total apparent surface area of sample *c* is 416 $m^2\ g^{-1}$ (cf. maximum of the curve corresponding to 1 Torr in Fig. 2A) it therefore follows that the increase in "external" surface area from sample *a* to sample *c* is responsible for less than 10% of the total increase observed. We will therefore first focus our attention, in the discussion, on the formation of the microporous structure.

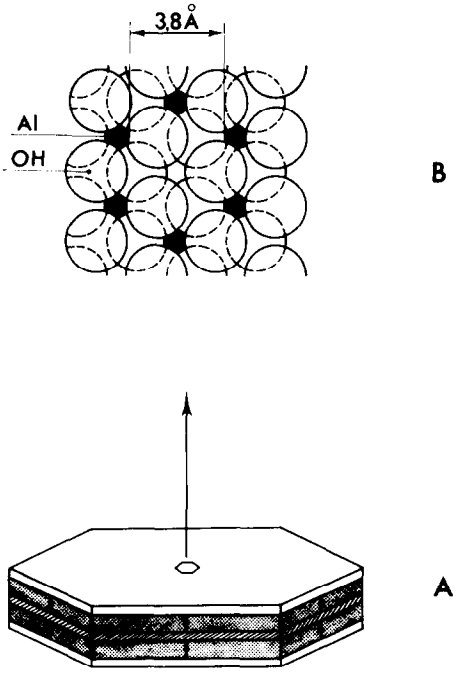

FIG. 4. (A) Advance of the dehydration interface in a gibbsite microcrystal. (B) Cross-sectional view of a "structural channel" lined with hydroxyls.

DISCUSSION

Our interpretation, mainly based on the one hand on the above experimental work and on the other hand on the work of de Boer *et al.* and of Papée and Tertian already mentioned, is fairly straightforward.

In Part I (*1*), we left the decomposition mechanism at the moment when the formation of boehmite was nearly over, because of the internal lowering of pressure (due either to a thinning of the gibbsite shell or to a cleavage of the crystallites). The representative point of the sample was the point b_1 on Fig. 1A.

From that point onwards we detect an apparent zero order of reaction: This is easily explained by a constant area reaction interface, advancing parallel to the large sides of the crystals, as is suggested in Fig. 4A. We know that this reaction creates micropores (cf. α_s plots) and that the surface area accessible to nitrogen in all our experiments increases linearly with the extent of decomposition. This leads us to assume that a number of micropores, normal to the reaction interface and therefore parallel to each other are left behind that interface, that number being unchanged during the whole reaction. This is also the orientation detected by de Boer *et al.* (*3, 4*) in their final product (treated at 245°C under atmospheric pressure) by a birefringence study. When the reaction interface reaches the boehmite core, all the gibbsite is already decom-

posed into amorphous or ρ alumina, depending on the residual pressure maintained (cf. Fig. 1C).

To explain this "drilling" of micropores into the gibbsite crystal we shall not make use of one of the "homogeneous" mechanisms formerly suggested, where the water loss was supposed to be uniform from all regions of the microcrystal (*15*), but instead we shall consider a "heterogeneous" one. We suggest that it involves two phenomena. The first one is the dehydroxylation of slightly less than one out of two of the "structural channels" already referred to in Part I (one of them is seen "from above" in Fig. 4B) and only lined with hydroxyls. This removal mainly needs a thermal motion of hydroxyls (allowing them to condense), the resulting distortion of the lattice (and the corresponding stored energy) being then favorable for a short range proton migration, in order to allow the departure of the last oxygen ions or hydroxyls lining the channel under consideration. These ideas are consistent with those recently developed by Freund *et al.* (*16*). From Fig. 4B we see that the basic micropore width would be 3.8 Å. Actually, it may be somewhat smaller, since our experiment at 2×10^{-4} Torr failed to develop any microporosity accessible to nitrogen. Anyway, the shape and size of the nitrogen molecule [length: 4.2 Å; width: 3.1 Å (*17*)] and its important quadrupole moment (which may block the entrance of micropores by a strong interaction between the nitrogen molecule and the outer ring of Al ions) do not allow us to be more accurate on that point.

The second phenomenon, which now explains the size of the micropores, is one in which the water vapor pressure plays a major part. Indeed, the water formed must leave the reaction interface at the bottom of the micropores. The smaller is the bottom diameter, the more difficult is the desorption. Conversely, if we control the water vapor pressure above the sample *and* if we want a given rate of decomposition, these conditions will dictate the diameter of the bottom of the micropores. The way to increase it beyond about 3.8 Å is to operate at a temperature at which a migration of Al ions may occur. This is automatically obtained with our C.R.T.A. equipment: We see for instance, from the recordings reproduced in Fig. 1A, that, when the pressure above the sample is increased from 0.04 to 1 Torr, the temperature of the sample is raised by nearly 30 K in order to insure the same rate of decomposition. The overall mechanism is then similar to the "inhomogeneous" mechanism suggested by Ball and Taylor (*18*) and also by Balmbra *et al.* (*19*) in the case of magnesium hydroxide. Nevertheless, as we saw, the migration of Al ions is only necessary to obtain wider pores than the basic structural channels emptied from their hydroxyls. We must also notice that the lattice of the alumina obtained at 0.04 Torr suffers strains and deformations (due to the water departure from nearly half of the "structural channels") which give an "amorphous" X-ray spectrum and a high differential enthalpy of dehydration (88, 84, and 80.5 kJ mol^{-1} for the 0.2, 1, and 50- to 80-μm samples, respectively) indicating that energy is stored in the strained structure. At 1 Torr, the slight migration of Al ions (by which we explain the larger diameter of micropores) restores a more ordered structure, giving rise to the one-peak X-ray spectrum of ρ alumina and to a lower differential enthalpy of dehydration for the three samples (80, 78.5, and 77 kJ mol^{-1}, respectively).

In our experiments (i.e., with control of the decomposition rate at a low level), the process of micropore formation appears to be only weakly controlled by diffusion of water along micropores: otherwise, the dehydration rate (or, in our case, the dehydration temperature) would change

significantly from b_1 to c (cf. Fig. 1A) as the depth of the micropores is increasing. Moreover it seems that, in our experimental conditions, nearly the whole mechanism takes place at the reaction interface; this is strikingly illustrated by the experiments reported in Fig. 2D which show that "funnel shaped" micropores may be drilled by lowering the pressure during the experiment: The smaller mean diameter of the micropores formed at 0.04 Torr means that, among them, a smaller proportion is accessible to nitrogen than among the micropores formed at 1 Torr. We may check that the mean diameter of the pores formed at 0.04 Torr (which is linked with the slope of the curve) is only weakly influenced by the existence of the slightly wider micropores already formed at 1 Torr. We may guess that a stronger influence of the desorption from the opening of the pores could be detected if we would carve ink-bottle-shaped micropores (unfortunately more difficult to prove than the funnel-shaped ones) by increasing the pressure during the experiment. The small part played by water diffusion through the already formed micropores is more easily understood with the two following remarks:

(a) In the experimental conditions corresponding to Figs. 2A and D (starting surface area: 5 $m^2\ g^{-1}$; rate of decomposition: 16 mg h^{-1} for a sample of 1.4 g) we calculate that the reaction interface is advancing at a rate of approximately 10 Å per hour, corresponding to the loss of only 12 water molecules per micropore and per hour.

(b) The fourfold increase of external surface area shown by the α_s plots from b_1 (7.5 $m^2\ g^{-1}$) to b_2 (28 $m^2\ g^{-1}$) may be explained by cracks but also by cleavages of the already decomposed part of the crystals, therefore shortening the micropores (we think that cleavages of the undecomposed part of the crystals would lead to a noticeable increase of the reaction rate, which is not observed). Lastly, the small differences observed both in Fig. 2A, when the pressure is increased from 1 to 5 Torr, and in Fig. 2B, when the decomposition rate is strongly changed at a constant pressure of 1 Torr, show us that at 1 Torr nearly all the micropores formed are accessible to nitrogen. Their mean diameter is then likely to be around 5 Å.

We think that the same mechanism holds for the decomposition of crude industrial gibbsite: We record similar thermal analysis curves, with the same apparent zero order (cf. Fig. 4 in Part I), and we saw that the surface area development seems to follow the same law (cf. Fig. 2C); we must nevertheless take into consideration that the pressure and decomposition rate conditions "seen" by each microcrystal in the gibbsite grain are more widely spread than in the case of a microcrystalline sample, especially if the gibbsite grain is submitted to a conventional heat treatment with no control of residual pressure nor of decomposition rate. For instance, a locally high decomposition rate will enhance a splitting of the elementary microcrystals (along the cleavage planes mainly), leading to the slit-shaped pores observed by de Boer *et al.* (*3*, *4*).

REFERENCES

1. Rouquerol, J., Rouquerol, F., and Ganteaume, M., *J. Catal.* **36**, 99 (1975).
2. de Boer, J. H., Fortuin, J. M. H., and Steggerda, J. J., *Proc. Kon. Ned. Akad. Wetensch. Ser. B* **57**, 170, 434 (1954).
3. de Boer, J. H., Steggerda, J. J., and Zwietering, P., *Proc. Kon. Ned. Akad. Wetensch. Ser. B* **59**, 435 (1956).
4. de Boer, J. H., van den Heuvel, A., and Linsen, B. G., *J. Catal.* **3**, 268 (1964).
5. Tertian, R., Papée, D., and Charrier, J., *C. R. Acad. Sci.* **238**, 98 (1954).
6. Papée, D., and Tertian, R., *Bull. Soc. Chim. Fr.* 983 (1955).
7. Eyraud, C., and Goton, R., *J. Chim. Phys. Physicochim. Biol.* **51**, 430 (1954).

8. Rouquerol, J., *J. Therm. Anal.* **2**, 123 (1970).
9. Rouquerol, J., *Bull. Soc. Chim. Fr.* 31 (1964).
10. Paulik, F., and Paulik, J., *Thermochim. Acta* **4**, 189 (1972).
11. Rouquerol, J., *in* "Thermal Analysis," (R. F. Schwenker, Jr., and P. O. Garn, Eds.), p. 281. Academic Press, New York, 1969.
12. Rouquerol, J., *J. Therm. Anal.* **5**, 203 (1973).
13. Sing, K. S. W., *in* "Surface Area Determination Proc. Internation. Symp. Bristol, 1969," p. 25. Butterworths, London, 1970.
14. Lippens, B. C., and de Boer, J. H., *J. Catal.* **4**, 319 (1965).
15. Dent Glasser, L. S., Glasser, F. P., and Taylor, H. F. W., *Quart. Rev.* **16**, 343 (1962).
16. Freund, F., Gieseke, W., and Nagerl, H., *in* "Reaction Kinetics in Heterogeneous Chemical Systems," (P. Barret, Ed.), p. 258. Elsevier, Amsterdam/Oxford/NewYork, 1975.
17. Pierce, C., and Ewing, B., *J. Phys. Chem.* **68**, 2562 (1964).
18. Ball, M. C., and Taylor, H. F. W., *Mineral. Mag.* **32**, 754 (1961).
19. Balmbra, R. R., Clunie, J. S., and Goodman, J. F., *Nature* **209**, 1083 (1966).
20. Ganteaume, M., and Rouquerol, J., *J. Therm. Anal.* **3**, 413 (1971).